# Reduction of Bias in Maximum Likelihood Ellipse Fitting *

Bogdan Matei Peter Meer
Electrical Engineering Department, Rutgers University
94 Brett Road, Piscataway, NJ 08854, USA
matei,meer caip.rutgers.edu

## Abstract

*An improved maximum likelihood estimator for ellipse fitting based on the heteroscedastic errors-in-variables (HEIV) regression algorithm is proposed. The technique significantly reduces the bias of the parameter estimates present in the Direct Least Squares method, while it is numerically more robust than renormalization, and requires less computations than minimizing the geometric distance with the Levenberg-Marquardt optimization procedure. The HEIV algorithm also provides closed-form expressions for the covariances of the ellipse parameters and corrected data points. The quality of the different solutions is assessed by defining confidence regions in the input domain, either analytically, or by bootstrap. The latter approach is exclusively data driven and it is used whenever the expression of the covariance for the estimates is not available.*

**Keywords:** errors-in-variables models, heteroscedastic noise, maximum likelihood estimation, bootstrap, confidence regions.

## 1. Introduction

Let $\boldsymbol{x}_{io} \in \mathbb{R}^2$, $i = 1 \cdots n$ be the true values of the image points assumed to obey the quadratic model

$$\varphi(\boldsymbol{x}_{io},\, \boldsymbol{Q},\, \boldsymbol{c}) = (\boldsymbol{x}_{io} - \boldsymbol{c})^\top \boldsymbol{Q} (\boldsymbol{x}_{io} - \boldsymbol{c}) - 1 = 0 \qquad (1)$$

where $\boldsymbol{c}$ is the center of ellipse and $\boldsymbol{Q}$ is a positive definite $2 \times 2$ matrix defining the shape of the ellipse. Throughout the paper the subscript '$o$' denotes the true, unknown values of the data. The true values $\boldsymbol{x}_{io}$ are corrupted by additive noise

$$\boldsymbol{x}_i = \boldsymbol{x}_{io} + \delta \boldsymbol{x}_i \qquad \delta \boldsymbol{x}_i \sim GI(\boldsymbol{0},\, \sigma^2 \boldsymbol{C}_{x_i}) \qquad (2)$$

where $\boldsymbol{x}_i$ are independent variables and $GI(\boldsymbol{\mu},\, \boldsymbol{C})$ stands for a general and distribution with mean $\boldsymbol{\mu}$ and covariance $\boldsymbol{C}$. It is assumed that the covariance matrices $\boldsymbol{C}_{x_i}$ are known up to a common multiplicative factor, the noise variance $\sigma^2$.

*The support of the NSF grants IRI-9530546 and IIS-9872995 is gratefully acknowledged.

Equation (1) can be expressed equivalently in the linearized form [4, 7, 10]

$$\varphi(\boldsymbol{x}_{io},\, \alpha,\, \boldsymbol{\theta}) = \alpha + \boldsymbol{z}(\boldsymbol{x}_{io})^\top \boldsymbol{\theta} = 0 \qquad (3)$$

where $\boldsymbol{z}(\boldsymbol{x}_{io})$ are the *carriers* dependent only on the data

$$\boldsymbol{z}_{io} = \boldsymbol{z}(\boldsymbol{x}_{io}) = [\; x_{1io} \quad x_{2io} \quad x_{1io}x_{2io} \quad x_{1io}^2 \quad x_{2io}^2 \;] \qquad (4)$$

and $\alpha$ and the five-dimensional $\boldsymbol{\theta}$ are the linearized ellipse parameters

$$\alpha = \boldsymbol{c}^\top \boldsymbol{Q} \boldsymbol{c} \quad \boldsymbol{\theta} = [-2\boldsymbol{c}^\top \boldsymbol{Q} \quad 2Q^{(12)} \quad Q^{(11)} \quad Q^{(22)}]\,. \qquad (5)$$

To have (3) represent an ellipse, the parameter $\boldsymbol{\theta}$ must satisfy the additional *ancillary* constraint [4]

$$4\theta_4\theta_5 - \theta_3^2 = 4(Q^{(11)}Q^{(22)} - (Q^{(12)})^2) > 0\,. \qquad (6)$$

Since $\alpha$ and $\boldsymbol{\theta}$ need to be known only up to a multiplicative constant, (6) can be written as

$$4\theta_4\theta_5 - \theta_3^2 = 1\,. \qquad (7)$$

In the Direct Least Squares (DLS) method proposed by Fitzgibbon et al. [4] the noniterative solution $\{\hat{\alpha},\, \hat{\boldsymbol{\theta}}\}$ is found by minimizing the squared algebraic distances

$$[\hat{\alpha},\, \hat{\boldsymbol{\theta}}] = \arg\min_{\alpha,\, \theta} \sum_{i=1}^{n} (\alpha + \boldsymbol{z}_i^\top \boldsymbol{\theta})^2 \quad \boldsymbol{z}_i = \boldsymbol{z}(\boldsymbol{x}_i) \qquad (8)$$

subject to (7).

The technique is equivalent to a Total Least Squares (TLS) estimation [14] which is consistent (the estimates converge asymptotically to the true values) *only when* the noise affecting the carriers $\delta \boldsymbol{z}_i$ satisfies

$$\delta \boldsymbol{z}_i \sim GI(\boldsymbol{0},\, \sigma^2 \boldsymbol{I}_5)\,. \qquad (9)$$

However, it can be easily shown by Taylor expansion of the carriers $\boldsymbol{z}(\boldsymbol{x}_i)$ around the true values $\boldsymbol{x}_{io}$ that $\delta \boldsymbol{z}_i \sim GI(\boldsymbol{\mu}_{z_i},\, \sigma^2 \boldsymbol{C}_{z_i})$ with

$$\boldsymbol{\mu}_{z_i} = [\; 0 \quad 0 \quad \sigma^2 C_{x_i}^{(12)} \quad \sigma^2 C_{x_i}^{(11)} \quad \sigma^2 C_{x_i}^{(22)} \;]^\top \qquad (10)$$

$$\boldsymbol{C}_{z_i} = \left[\frac{\partial \boldsymbol{z}_i}{\partial \boldsymbol{x}_{io}}\right] \boldsymbol{C}_{x_i} \left[\frac{\partial \boldsymbol{z}_i}{\partial \boldsymbol{x}_{io}}\right]^\top \quad \frac{\partial \boldsymbol{z}_i}{\partial \boldsymbol{x}_{io}} = \begin{bmatrix} 1 & 0 \\ 0 & 1 \\ x_{2io} & x_{1io} \\ 2x_{1io} & 0 \\ 0 & 2x_{2io} \end{bmatrix} \qquad (11)$$

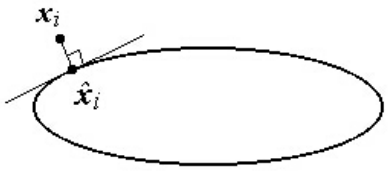


**Figure 1. Minimization of the geometric distance from the measurements to the ellipse.**

The DLS estimates are significantly biased when the available measurements come from short ellipse segments with low curvature. The approach, however, has the advantage of yielding a noniterative solution and automatically imposing the ellipse constraint (7).

The Maximum Likelihood (ML) estimator under normal noise $\delta \boldsymbol{x}_i$ for $\alpha,\ \boldsymbol{\theta}$ and $\boldsymbol{x}_{1o}, \cdots, \boldsymbol{x}_{no}$ is

$$[\hat{\alpha},\, \hat{\boldsymbol{\theta}},\, \hat{\boldsymbol{x}}_i] = \arg \min_{\alpha,\, \boldsymbol{\theta},\, \boldsymbol{x}_{io}} \sum_{i=1}^{n} (\boldsymbol{x}_i - \boldsymbol{x}_{io})^{\mathsf{T}} \boldsymbol{C}_{x_i}^{-} (\boldsymbol{x}_i - \boldsymbol{x}_{io}) \quad (12)$$

subject to (3) and (7). There are $n+2$ unknowns $\alpha$, $\boldsymbol{\theta}$, $\boldsymbol{x}_{io}$, $i = 1 \cdots n$, but only $n$ available measurements $\boldsymbol{x}_i$.

A way of reducing the number of unknowns in ML estimation is to restrict the *corrected* measurements $\hat{\boldsymbol{x}}_i$ (the estimators of the true values $\boldsymbol{x}_{io}$) to the projection of $\boldsymbol{x}_i$ onto the ellipse $\hat{\alpha},\ \hat{\boldsymbol{\theta}}$, as shown in Figure 1. The criterion (12) then becomes the minimization of the sum of geometric distances from $\boldsymbol{x}_i$ to $\hat{\boldsymbol{x}}_i$ under the metric induced by $\boldsymbol{C}_{x_i}$. The solution of this nonlinear problem is usually obtained with the Levenberg-Marquardt (L-M) technique. The approach is computationally intensive, since it requires at each iteration step finding the roots of a four-degree polynomial for every point $\boldsymbol{x}_i$ [15]. To reduce the amount of computation the geometric distances are often approximated by Taylor expansion [5, pp.230–244][13] at the price of introducing a small bias in the estimates.

## 2. HEIV Estimator for Ellipse Fitting

The improved ML algorithm for solving the linearized model (3) is presented next. The approach extends [10, 11] using the results from [1]. As was shown in Section 1 the carriers are corrupted by noise dependent on the measurements $\boldsymbol{x}_i$, i.e., *heteroscedastic* noise. Since the errors corrupting the true values $\boldsymbol{x}_{io}$ appear inside the carriers $\boldsymbol{z}_i$, (3) is called an *errors-in-variables* (EIV) model [1][5, pp.30–31]. An excellent introduction to EIV nonlinear models is [5]. The heteroscedastic EIV (HEIV) algorithm introduced below exploits the linear dependency of (3) in $\alpha$, $\boldsymbol{\theta}$ and iteratively solves a generalized eigenproblem. The first and second order moments of the carrier noise $\delta \boldsymbol{z}_i$ are also updated during the iterations. The quality of the HEIV estimates can be assessed by the covariance matrices and confidence regions provided.

### 2.1. HEIV Algorithm

The update rules for the HEIV algorithm are summarized below. The iteration index is dropped for simplicity.

1) Start with an initial random $\hat{\boldsymbol{\theta}}^{(0)}$. Evaluate $\boldsymbol{C}_{z_i}$ at $\boldsymbol{x}_i$ using (11) and let $\boldsymbol{\mu}_{z_i} = \boldsymbol{0}$. Alternatively, $\hat{\boldsymbol{\theta}}^{(0)}$ may be a TLS estimate obtained by taking $\boldsymbol{C}_{z_i} = \boldsymbol{I}_5$ and $\boldsymbol{\mu}_{z_i} = \boldsymbol{0}$. Let $\boldsymbol{z}_i' = \boldsymbol{z}_i$.
2) Compute

$$\hat{\xi}_i = \hat{\boldsymbol{\theta}}^{\mathsf{T}} \boldsymbol{C}_{z_i} \hat{\boldsymbol{\theta}} \qquad i = 1 \cdots n \quad (13)$$

Calculate the weighted centroid of the carriers

$$\tilde{\boldsymbol{z}} = \left[ \sum_{i=1}^{n} \hat{\xi}_i^{-1} \right]^{-1} \sum_{i=1}^{n} \hat{\xi}_i^{-1} \boldsymbol{z}_i' \,. \quad (14)$$

3) Calculate the scatter matrix

$$\boldsymbol{S}[\hat{\boldsymbol{\theta}}] = \sum_{i=1}^{n} \hat{\xi}_i^{-1} [\boldsymbol{z}_i' - \tilde{\boldsymbol{z}}][\boldsymbol{z}_i' - \tilde{\boldsymbol{z}}]^{\mathsf{T}} \quad (15)$$

and the weighted covariance matrix

$$\boldsymbol{C}[\hat{\boldsymbol{\theta}}] = \sum_{i=1}^{n} \nu_i^2 \boldsymbol{C}_{z_i} \quad \nu_i = \hat{\xi}_i^{-1} (\boldsymbol{z}_i' - \tilde{\boldsymbol{z}})^{\mathsf{T}} \hat{\boldsymbol{\theta}} \,. \quad (16)$$

Note that $\boldsymbol{S}[\hat{\boldsymbol{\theta}}]$ and $\boldsymbol{C}[\hat{\boldsymbol{\theta}}]$ are positive semidefinite.
4) Compute the new $\hat{\boldsymbol{\theta}}$ as the smallest unit eigenvector (the eigenvector corresponding to the smallest eigenvalue) of the generalized eigenproblem

$$\boldsymbol{S}[\hat{\boldsymbol{\theta}}]\, \hat{\boldsymbol{\theta}} = \lambda \boldsymbol{C}[\hat{\boldsymbol{\theta}}]\, \hat{\boldsymbol{\theta}} \,. \quad (17)$$

Compute the new intercept

$$\hat{\alpha} = -\tilde{\boldsymbol{z}}^{\mathsf{T}} \hat{\boldsymbol{\theta}} \,. \quad (18)$$

5) Update the corrected measurements $\hat{\boldsymbol{x}}_i$

$$\hat{\boldsymbol{x}}_i = \boldsymbol{x}_i - \hat{\xi}_i^{-1} \varphi(\boldsymbol{x}_i,\, \hat{\alpha},\, \hat{\boldsymbol{\theta}}) \boldsymbol{C}_{x_i} \left[ \frac{\partial \boldsymbol{z}_i}{\partial \hat{\boldsymbol{x}}_i} \right]^{\mathsf{T}} \hat{\boldsymbol{\theta}} \,. \quad (19)$$

6) Update the noise variance estimate

$$\hat{\sigma}^2 = \frac{\hat{\boldsymbol{\theta}}^{\mathsf{T}} \boldsymbol{S}[\hat{\boldsymbol{\theta}}]\, \hat{\boldsymbol{\theta}}}{n-4} \,. \quad (20)$$

7) Update the moments of the carrier noise

$$\boldsymbol{\mu}_{z_i} = [\, 0 \quad 0 \quad \hat{\sigma}^2 C_{x_i}^{(12)} \quad \hat{\sigma}^2 C_{x_i}^{(11)} \quad \hat{\sigma}^2 C_{x_i}^{(22)} \,]^{\mathsf{T}} \quad (21)$$

$$\boldsymbol{C}_{z_i} = \left[ \frac{\partial \boldsymbol{z}_i}{\partial \hat{\boldsymbol{x}}_i} \right] \boldsymbol{C}_{x_i} \left[ \frac{\partial \boldsymbol{z}_i}{\partial \hat{\boldsymbol{x}}_i} \right]^{\mathsf{T}} \,. \quad (22)$$

8) Update

$$\boldsymbol{z}_i' = \boldsymbol{z}_i - \boldsymbol{\mu}_{z_i} \quad i = 1 \cdots n \quad (23)$$

9) Go to step 2 until the smallest eigenvalue $\lambda = 1$.

The first-order renormalization technique of Kanatani for linearized models [8, pp.267–290] is a particular case of the HEIV algorithm, obtained by substituting in (16) $\boldsymbol{\mu}_{z_i} = \mathbf{0}$ and

$$\boldsymbol{C}[\hat{\boldsymbol{\theta}}] = \sum_{i=1}^{n} \xi_i^{-1} \boldsymbol{C}_{z_i} . \tag{24}$$

The covariance matrices of the carriers are evaluated at the noisy measurements $\boldsymbol{x}_i$ and are not updated during the iterations. The renormalization iterates $\hat{\boldsymbol{\theta}}$ as the smallest eigenvector of $\boldsymbol{S}[\hat{\boldsymbol{\theta}}] - \boldsymbol{C}[\hat{\boldsymbol{\theta}}]$. We have found that solving the generalized eigenvalue problem (17) at Step 4 yields faster convergence and less dependence on the initial $\hat{\boldsymbol{\theta}}^{(0)}$. The second-order renormalization algorithm [8, pp.290–294] takes the bias of the carriers $\boldsymbol{\mu}_{z_i}$ also into consideration by using second order Taylor expansion, but the analysis becomes quite involved.

### 2.2. Statistical Properties of HEIV Estimates

Up to a first order approximation all the HEIV estimates are unbiased. The covariance of the corrected points $\hat{\boldsymbol{x}}_i$ given $\hat{\boldsymbol{\theta}}$ is the rank-one matrix

$$\boldsymbol{C}_{\hat{x}_i|\hat{\theta}} = \boldsymbol{C}_{x_i} - \hat{\xi}_i^{-1} \boldsymbol{C}_{x_i} \left[ \frac{\partial \boldsymbol{z}_i}{\partial \hat{\boldsymbol{x}}_i} \right]^{\top} \hat{\boldsymbol{\theta}} \hat{\boldsymbol{\theta}}^{\top} \left[ \frac{\partial \boldsymbol{z}_i}{\partial \hat{\boldsymbol{x}}_i} \right] \boldsymbol{C}_{x_i} . \tag{25}$$

The covariance of $\hat{\boldsymbol{\beta}}^{\top} = [\ \hat{\alpha} \quad \hat{\boldsymbol{\theta}}^{\top}\ ]$ is obtained from the perturbation theory of the eigenvectors [9, pp.72–99]

$$\boldsymbol{C}_{\hat{\beta}} = \begin{bmatrix} \tilde{\boldsymbol{z}}^{\top} \boldsymbol{C}_{\hat{\theta}} \tilde{\boldsymbol{z}} & -\tilde{\boldsymbol{z}}^{\top} \boldsymbol{C}_{\hat{\theta}} \\ -\boldsymbol{C}_{\hat{\theta}} \tilde{\boldsymbol{z}} & \boldsymbol{C}_{\hat{\theta}} \end{bmatrix} , \quad \text{where} \tag{26}$$

$$\boldsymbol{C}_{\hat{\theta}} = \hat{\sigma}^2 \left[ \boldsymbol{S}[\hat{\boldsymbol{\theta}}] - \boldsymbol{C}[\hat{\boldsymbol{\theta}}] \right]^{-} . \tag{27}$$

Assuming that the HEIV algorithm has converged, the matrix $\boldsymbol{S}[\hat{\boldsymbol{\theta}}] - \boldsymbol{C}[\hat{\boldsymbol{\theta}}]$ has rank four, and therefore the pseudoinverse must be used in (27).

### 2.3. Imposing the Ancillary Constraint

When the constraint (7) is not satisfied a $\hat{\hat{\boldsymbol{\theta}}}$ has to be found such that [4]

$$\hat{\hat{\boldsymbol{\theta}}}^{\top} \boldsymbol{D} \hat{\hat{\boldsymbol{\theta}}} = 1 \quad \boldsymbol{D} = \begin{bmatrix} 0 & 0 & 0 & 0 & 0 \\ 0 & 0 & 0 & 0 & 0 \\ 0 & 0 & -1 & 0 & 0 \\ 0 & 0 & 0 & 0 & 2 \\ 0 & 0 & 0 & 2 & 0 \end{bmatrix} . \tag{28}$$

The solution is obtained from

$$\hat{\hat{\boldsymbol{\theta}}} = \arg\min_{\theta} \left\{ (\boldsymbol{\theta} - \hat{\boldsymbol{\theta}})^{\top} \boldsymbol{C}_{\hat{\theta}}^{-} (\boldsymbol{\theta} - \hat{\boldsymbol{\theta}}) - \eta (\boldsymbol{\theta}^{\top} \boldsymbol{D} \boldsymbol{\theta} - 1) \right\} \tag{29}$$

with $\boldsymbol{C}_{\hat{\theta}}$ defined in (27). Taking the derivative of (29) with respect to $\boldsymbol{\theta}$ and using (27) we find

$$\left[ \boldsymbol{S}[\hat{\boldsymbol{\theta}}] - \boldsymbol{C}[\hat{\boldsymbol{\theta}}] \right] \hat{\hat{\boldsymbol{\theta}}} = \eta \boldsymbol{D} \hat{\hat{\boldsymbol{\theta}}} . \tag{30}$$

The DLS estimate corresponds to substituting in (30) $\boldsymbol{S}[\hat{\boldsymbol{\theta}}]$ and $\boldsymbol{C}[\hat{\boldsymbol{\theta}}]$ with

$$\boldsymbol{S} = \sum_{i=1}^{n} [\boldsymbol{z}_i - \tilde{\boldsymbol{z}}][\boldsymbol{z}_i - \tilde{\boldsymbol{z}}]^{\top} \quad \tilde{\boldsymbol{z}} = \frac{1}{n} \sum_{i=1}^{n} \boldsymbol{z}_i \quad \boldsymbol{C} = \mathbf{0} . \tag{31}$$

In this case, it can be proven using Sylvester's law of inertia, that only one finite positive eigenvalue exists [4]. The estimate $\hat{\hat{\boldsymbol{\theta}}}$ is then the eigenvector corresponding to this eigenvalue. However, since $\boldsymbol{S}[\hat{\boldsymbol{\theta}}] - \boldsymbol{C}[\hat{\boldsymbol{\theta}}]$ is *singular* in the HEIV algorithm, the inertia law doesn't hold for (30), and the signs of the eigenvalues cannot be a priori specified. The minimum error in (29) corresponds to the eigenvector corresponding to the smallest nonnegative eigenvalue, if it exists. When such an eigenvalue doesn't exist, the fall back method is to use the DLS estimate, which always can be found.

## 3. Confidence Regions for the Parameters

The accuracy of an estimator can be assessed using statistical measures like covariance matrices and confidence regions. As was shown in Section 2.2, the HEIV estimates $\hat{\boldsymbol{x}}_i$ and $\hat{\boldsymbol{\beta}}$ are unbiased and have the covariance matrices (25), respectively (26). An elliptical confidence region $\mathcal{D}_{\hat{\beta}}$ for $\hat{\boldsymbol{\beta}}$ can be constructed in the six-dimensional parameter space assuming that $\hat{\boldsymbol{\beta}}$ has a normal distribution [12], however the visualization of $\mathcal{S}_{\hat{\beta}}$ in the input space is desirable.

In the case of estimators for which closed-form expression of the covariance $\boldsymbol{C}_{\hat{\beta}}$ is not available, the confidence region of an estimate can be found with the bootstrap methodology [11, 12].

### 3.1. Confidence Regions for HEIV Estimates

The visualization in the input space of the confidence region $\mathcal{D}_{\hat{\beta}}$ associated with the covariance matrix $\boldsymbol{C}_{\hat{\beta}}$ is achieved in [8, pp.122–124] using the *primary deviation pairs* which are determined by the largest eigenvector of $\boldsymbol{C}_{\hat{\beta}}$. A more accurate method, however, can be used [2, pp.334–335] as shown in Figure 2.

Given an ellipse $\hat{\boldsymbol{\beta}}$, for any $x_1 \in \mathbb{R}$, there are two real or imaginary values $x_{2d}$ and $x_{2u}$, $x_{2u} > x_{2d}$ such that (4) $\boldsymbol{z}_d = \boldsymbol{z}(x_1, x_{2d})$, $\boldsymbol{z}_u = \boldsymbol{z}(x_1, x_{2u})$ satisfy the ellipse constraint

$$\hat{\alpha} + \boldsymbol{z}_d^{\top} \hat{\boldsymbol{\theta}} = 0 \quad \hat{\alpha} + \boldsymbol{z}_u^{\top} \hat{\boldsymbol{\theta}} = 0 \qquad \|\hat{\boldsymbol{\theta}}\| = 1 . \tag{32}$$

Suppose that $x_{2u} \in \mathbb{R}$. Then, with confidence $1 - \gamma$

$$\alpha + \boldsymbol{z}_u^{\top} \boldsymbol{\theta} \in \left[ -\sqrt{\chi^2_{5,1-\gamma}}\, \sigma_u \quad \sqrt{\chi^2_{5,1-\gamma}}\, \sigma_u \right] \tag{33}$$

$$\|\boldsymbol{\theta}\| = 1 \quad \sigma_u^2 = [\,1 \quad \boldsymbol{z}_u^{\top}\,]\, \boldsymbol{C}_{\hat{\beta}}\, [\,1 \quad \boldsymbol{z}_u^{\top}\,]^{\top} \tag{34}$$

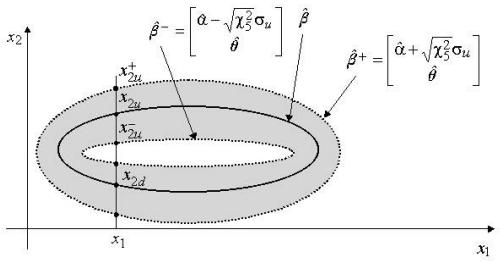


**Figure 2. Mapping of the confidence region $\mathcal{D}_{\hat{\beta}}$ of the ellipse estimate into the input domain.**

where $\chi^2_{v,1-\gamma}$ denotes the $1-\gamma$ quantile of the $\chi^2$ distribution with $v$ degrees of freedom. A similar expression is obtained for $\alpha + \boldsymbol{z}_d^\top \boldsymbol{\theta}$.

### 3.2. Bootstrap Confidence Regions

The bootstrap is a well-established technique to compute statistical measures for estimators using computer simulations with *resampled* data [3]. To illustrate this procedure, confidence regions for the DLS ellipse estimates are constructed.

The corrected measurements $\hat{\boldsymbol{x}}_i$ and their covariance matrices (25) returned by the HEIV algorithm are employed together with $\boldsymbol{x}_i$ and $\boldsymbol{C}_{x_i}$ in the generation of new *bootstrap samples* $\{\, \boldsymbol{x}_1^{*b} \cdots \boldsymbol{x}_n^{*b} \}$, $b = 1 \cdots B$ using the bootstrap of residuals [11]. For each bootstrap sample, the *bootstrap replicates* $\hat{\boldsymbol{\beta}}^{*b}$ are computed (using DLS algorithm this time) and employed subsequently for computing the covariance matrix $\boldsymbol{C}_{\hat{\beta}}$ and confidence region $\mathcal{D}_{\hat{\beta}}$ for the DLS estimate [12].

## 4. Experiments

Four algorithms: DLS, HEIV, renormalization and the geometric distance minimized with L-M were compared using synthetic and real data. The DLS estimates are generally biased when the available data comes from short ellipse segments with a low curvature, as illustrated in Figure 3. The L-M, though theoretically unbiased, may yield biased $\hat{\boldsymbol{\beta}}$ when its initialization, most often done using DLS, is far from the true value $\boldsymbol{\beta}$.

To assess the accuracy of the solutions yielded by these ellipse estimators, the true values $\boldsymbol{x}_{io}$ were selected from different segments of the ellipse

$$\boldsymbol{Q} = \begin{bmatrix} 1 & 0 \\ 0 & 4 \end{bmatrix} \qquad \boldsymbol{c} = \begin{bmatrix} 0 \\ 0 \end{bmatrix}.$$

Normal noise $\delta \boldsymbol{x}_i$ with zero mean and covariance $\boldsymbol{C}_{x_i} = \sigma^2 \boldsymbol{I}_2, \sigma = 0.02$ was added on the $n = 80$ true values, shown in Figure 4.

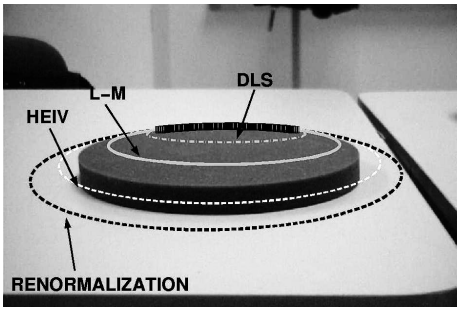


**Figure 3. The four ellipse estimators used in the experiments. The 218 data points $\boldsymbol{x}_i$ are highlighted in the back.**

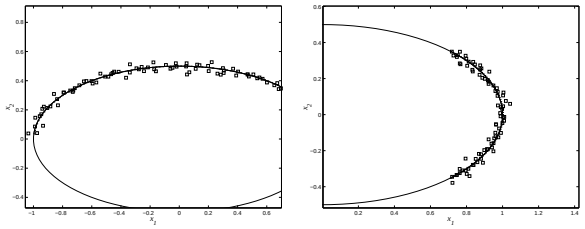

(a) (b)

**Figure 4. Synthetic data. Normal noise with zero-mean and covariance $0.02^2 \boldsymbol{I}_2$ was added on the $n = 80$ true values $\boldsymbol{x}_{io}$.**

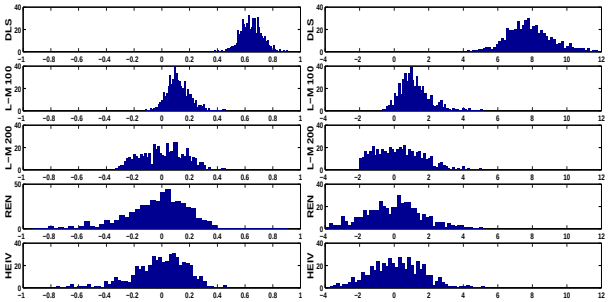


**Figure 5. Histogram of the estimation error for $Q^{(11)}$ (left) and for $Q^{(22)}$ (right) using the synthetic data from Figure 4 (a). 500 trials.**

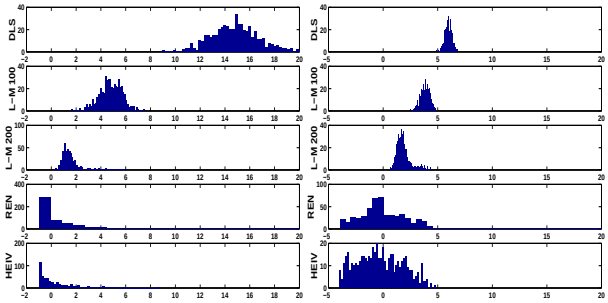


**Figure 6. Histogram of the estimation error for $Q^{(11)}$ (left) and for $Q^{(22)}$ (right) using the synthetic data from Figure 4 (b). 500 trials.**

The histograms of errors in the estimation of $Q^{(11)}$ and $Q^{(22)}$ using 500 Monte Carlo trials are presented in Figures 5 and 6. The DLS had the smallest spread, however, it was strongly biased. The MATLAB implementation of the L-M algorithm was used in the simulations. Note in Figures 5 and 6 how the bias in estimating $Q^{(11)}$ and $Q^{(22)}$ was reduced after 100 and 200 L-M iterations.

For the data from Figure 4 (a) the HEIV required about four iterations to reach convergence ($\lambda = 1$ with tolerance $10^{-8}$). The HEIV estimate $\hat{\boldsymbol{\beta}}$ satisfied the ancillary constraint (6) in all 500 trials. The renormalization required about six iterations to reach convergence (same tolerance for the eigenvalue) and in 3 trials the ancillary constraint (6) had to be imposed. The HEIV and the renormalization are unbiased, with the latter having a slightly larger spread.

The data from Figure 4 (b) leads to a more difficult estimation process since it comes from a shorter ellipse segment. The L-M remained biased even after 200 iterations. The ancillary constraint had to be imposed in 72 trials for HEIV and in 108 trials for the renormalization. Both algorithms required more iterations to converge (about seven for HEIV and ten for renormalization). Note again the larger spread of the estimates yielded by the renormalization compared with HEIV.

The confidence regions $\mathcal{D}_{\hat{\beta}}$ for the HEIV and DLS estimates constructed using the technique from Section 3 are presented in Figure 7. The covariance matrices $\boldsymbol{C}_{\hat{\beta}}$ were computed using (26) for HEIV and $B = 200$ bootstrap replicates $\hat{\boldsymbol{\beta}}^*$ for DLS. To assess the accuracy of $\mathcal{D}_{\hat{\beta}}$, derived analytically for HEIV, 200 bootstrap replicates were also calculated. Note from Figure 7 (a) the symmetric distribution of these replicates around $\hat{\boldsymbol{\beta}}$ (zero-bias) and inside the theoretical confidence region. On the other hand, the DLS bootstrap replicates are not symmetrically distributed, suggesting a biased estimate.

## 5. Conclusion

An improved ML ellipse estimator based on the HEIV algorithm is presented. Closed-form expressions for the covariance of the HEIV estimates are provided. Confidence regions of the ellipse estimates are constructed either analitically, or by bootstrap. The mapping in the input space of these confidence regions allows an easier assessment of the reliability of the solution yielded.

## References


[1] Y. Amemiya, "Generalization of the TLS Approach in Errors-Variables Problem", *Recent Advances in Total Least Squares Techniques and Errors-In-Variables Modeling*, pp. 77–86, SIAM, 1997.

[2] L. Breiman, *Statistics: With a View Toward Applications*, Houghton Mifflin Company, 1973.

[3] B. Efron, R.J. Tibshirani, *An Introduction to the Bootstrap*, Chapman&Hall, 1993.


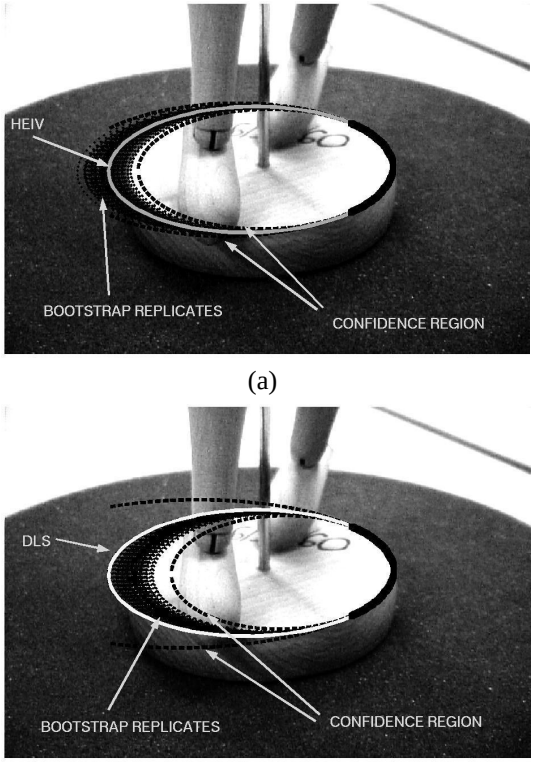


**Figure 7. Confidence regions for the estimates: (a) HEIV - obtained analitically and with bootstrap; (b) DLS - obtained with bootstrap. The 153 data points $\boldsymbol{x}_i$ used are on the highlighted segment on the right.**


[4] A. Fitzgibbon, M. Pilu, R.B. Fisher, "Direct least Square Fitting of Ellipses", *IEEE Trans. on PAMI*, vol. 21, pp. 476–480, 1999.

[5] W. Fuller, *Measurement Error Models*, John Wiley & Sons, 1987.

[6] J. Hornegger, C. Tomasi, "Representation Issues in the ML Estimation of Camera Motion", *Proc. 7th ICCV*, Kerkyra-Greece, pp. 640–647, 1999.

[7] K. Kanatani, "Statistical Bias of Conic Fitting and Renormalization", *IEEE Trans. on PAMI*, vol. 16, pp. 320-326, 1994.

[8] K. Kanatani, *Statistical Optimization for Geometric Computation: Theory and Practice*, Elsevier, 1996.

[9] T. Kato, *A Short Introduction to Perturbation Theory for Linear Operators*, Springer-Verlag, 1982.

[10] Y. Leedan, P. Meer, "Estimation with bilinear constraints in computer vision," *Proc. 6th ICCV*, Bombay, India, pp. 733–738, January 1998.

[11] B. Matei, P. Meer, ''Optimal rigid motion estimation and performance evaluation with bootstrap", *Proc. of CVPR '99*, Fort Collins CO., pp. 339–345, 1999.

[12] B. Matei, P. Meer, "Bootstrap for Errors-In-Variables", To appear in *Lecture Notes in Computer Science*, B. Triggs, R. Szeliski, A. Zisserman (Eds.), Springer, Spring 2000.

[13] G. Taubin, "An Improved Algorithm for Algebraic Curve and Surface Fitting", *IEEE Trans. on PAMI*, vol. 13, pp. 1115–1138, 1991.

[14] S. Van Huffel, Joos Vandewalle, *The Total Least Squares Problem. Computational Aspects and Analysis*, SIAM, 1991.

[15] Z. Zhang, "Parameter Estimation Techniques: A Tutorial with Application to Conic Fitting", *Image and Vision Computing*, vol. 15, pp. 59–76, 1997.